Seismic and Durability Assessment of Externally Bonded FRP Retrofits in Reinforced Concrete Structures After 2018 Anchorage, AK Earthquake

Sandra Milev[1], Shafique Ahmed[2], Mariam Hassan[3], Siamak Sattar[3], David Goodwin[3], and Jovan Tatar[1(✉)]

[1] University of Delaware, Newark, DE, USA
jtatar@udel.edu
[2] Echem Consultants LLC, Poughkeepsie, NY, USA
[3] National Institute of Standards and Technology, Gaithersburg, MD, USA

Abstract. Externally bonded fiber-reinforced polymer (EBFRP) composites are a cost-effective material used for repair and seismic retrofit of existing concrete structures. Even though EBFRP composites have been extensively utilized over the past 20 years as seismic retrofits, there are few data documenting their performance in a real shaking event or after long-term use on concrete structures. In this study, semi-destructive and non-destructive techniques were employed to evaluate the performance and durability of EBFRP-retrofitted buildings that had experienced the 2018 Cook Inlet Earthquake in Anchorage, AK. The performance of EBFRP was evaluated and documented through photographic evidence. Acoustic sounding, infrared thermography, and bond pull-off tests were utilized to evaluate the quality of bonding between the EBFRP and concrete. EBFRP samples were also collected from building interiors and exteriors for chemical and thermal analysis to evaluate the long-term effects of environmental exposure. Although environmental conditions were found to influence the bond quality between the EBFRP composite and concrete substrate, no major signs of earthquake damage to the building components retrofitted with EBFRP were noted. Materials characterization results demonstrated no evidence of polymer matrix degradation in exterior EBFRP samples.

Keywords: EBFRP retrofit · Seismic · Deterioration · Reconnaissance · Durability · Materials characterization

1 Introduction

Externally bonded fiber-reinforced polymer (EBFRP) composites provide effective solutions for rehabilitating and strengthening existing concrete structures that have suffered deterioration or require seismic retrofit. EBFRP composites possess several properties that make them an attractive retrofitting solution, including their lightweight, high strength, ability to conform to existing structural components geometries, and corrosion

A. Ilki et al. (Eds.): CICE 2021, LNCE 198, pp. 1216–1228, 2022.
https://doi.org/10.1007/978-3-030-88166-5_106

resistance. Over the past 30 years, there have been numerous publications to evaluate the effectiveness and benefits of EBFRP for the strengthening of reinforced concrete structural members. These studies showed that application of EBFRP composites can provide performance improvements including enhanced confinement and ductility, load-bearing capacity, blast resistance, and shear resistance (Bakis et al. 2002; Buchan and Chen 2007; He et al. 2015; Ma et al. 2016). However, there are not many data documenting performance of EBFRP in a real-world earthquake. Furthermore, the long-term performance of EBFRP is an issue that remains a concern in the engineering community (Goodwin et al. 2019). Evidence regarding the long-term performance of EBFRPs is currently based on limited short-term accelerated conditioning testing (Tatar and Hamilton 2014) without validation from real-world outdoor testing. Due to the effect of combined environmental conditions and factors, field exposure can result in different rates and mechanisms of degradation than those determined on the basis of controlled laboratory experiments. In addition, design recommendations, informed by laboratory experiments only, can result in overly-conservative designs that can negatively impact the cost-effectiveness of a retrofitting system (Zhang et al. 2014). Reports that describe the long-term performance of EBFRP composites in the field provide valuable information but are often limited by their use of a single type of material, a single retrofit configuration, a single outdoor exposure site, and the duration of the study. Some early projects and demonstrations have shown that EBFRP composites can have excellent durability characteristics in warm and cold climates for several years (Sheikh and Tam 2007; Steckel and Hawkins 2005). A field study conducted on carbon fiber reinforced polymer (CFRP)-wrapped girders that were taken out of service from bridges located in Florida indicated that bonded CFRP repairs can last upwards of 15 years and perhaps beyond with an EBFRP system applied to a well-prepared substrate surface (e.g., damaged concrete repaired if needed and surface treated to achieve the recommended ICRI surface profile (ICRI-No.03732 1997), using proper installation techniques that include full saturation, environmental conditions that do not affect epoxy cure, and removal of air voids by hand or with a trowel (Hamilton et al. 2017; Tatar et al. 2016). To contribute to existing field studies, this research project was initiated with an objective of evaluating field performance of EBFRP under earthquake loading and the effects of Alaska's subarctic climate on EBFRP durability.

2 Studied Buildings

Past seismic activity in Anchorage, AK led the community to retrofit many buildings over the years – some of them with EBFRP. During the 2018 Cook Inlet Earthquake, several buildings in Anchorage, AK retrofitted with EBFRP experienced shaking. For this reason, these buildings were visually inspected and two of them were selected for more detailed evaluation that is presented in this paper – the McKinley Tower (MKT) and Ted Stevens International Airport (TSIA). The epicenter of the earthquake that occurred on November 30th 2018 was 12 km north of Anchorage, AK. Based on the response spectra from several locations in Anchorage, AK, the 7.1 M_w earthquake had an intensity lower than the design earthquake. Most notable damage was caused by geotechnical failures that affected highways and many roads in the area. Reports of

post-earthquake inspection suggest that damage to the buildings was mostly limited to non-structural elements (StEER and EERI 2018).

MKT is a 36.6 m (120 ft) tall reinforced concrete residential building in Anchorage, constructed in 1951. The building was severely damaged in the 1964 Great Alaskan earthquake (M 9.2). After the earthquake, the building was abandoned and left unoccupied for approximately twenty years. It had fallen behind seismic codes and needed a retrofit before it could be reoccupied. A traditional retrofitting project was started in 1998 and then abandoned shortly thereafter because of its high cost. A new seismic evaluation was performed in 2004 when EBFRP was selected as a cost-effective solution to retrofit and strengthen the structure. Carbon and glass EBFRP retrofits, hereby referred to as CFRP and GFRP retrofits, respectively, were applied to columns, walls, and beams. The majority of the EBFRP retrofits were applied on floors 5 through 14 (Ehsani 2017).

Terminal 2 of TSIA was built in 1968 or later and seismically retrofitted in July 2008. The existing exterior columns in Terminal 2 were retrofitted to act as the boundary elements for the new shear walls. An interior column in a baggage handling area was also retrofitted. For both interior and exterior applications, CFRP was used to confine the columns.

During their lifetime, some of the outdoor EBFRP retrofits at MKT and TSIA were exposed to harsh environmental conditions typical for Anchorage, AK – average daytime summer temperatures from 12 °C to 25 °C, and average daytime winter temperatures in the −15 °C to 0 °C range, with an average relative humidity of 70% (National Oceanic and Atmospheric Administration 2020).

3 Experimental Program

3.1 Phase 1: Field Assessment

Prior to field assessment, data and information was collected about the buildings retrofitted with EBFRP in Anchorage, AK. The field assessment then took place in January 2019. All building inspections involved photographic evidence collection and further gathering of information related to EBFRP design documentation, details about EBFRP materials, and inspection reports from before and after the repair. Since the effectiveness of EBFRP strengthening depends on the properties of the bond between the concrete and EBFRP, a detailed evaluation of the EBFRP bond was conducted using acoustic sounding, infrared (IR) thermography, and bond pull-off tests at Ted Stevens International Airport and McKinley Tower.

Acoustic sounding and *Infrared (IR) thermography* were used to locate areas of EBFRP debonding from the concrete substrate (Reay and Pantelides 2006). Debonded areas detected by acoustic sounding, in this case—light tapping with a hammer—have a hollow sound upon hammer impact. After detection, hollow-sounding areas were marked with a blue tape and documented with photographs. For IR thermography, the surface of the EBFRP was evenly heated by a halogen lamp and the heat dissipation was measured using an IR thermography instrument from an approximately consistent distance. The technique works by detecting the slower heat dissipation through the debonded areas than through the areas that are properly bonded. The debonded areas show up as “hot spots” in an IR image. Although IR thermography is a useful tool to detect debonding,

the technique is time-consuming (*e.g.,* an hour or more per column face). For this reason, the IR thermography method was used only for one interior and one exterior column at TSIA. During post-processing of the IR thermography data, the size and shapes of the debonded areas were matched with the debonded areas identified with acoustic sounding. Acoustic sounding data was also used to identify "false positive" readings in the thermographs associated with the uneven thickness of the epoxy adhesive or EBFRP composite (Brown 2005).

Bond pull-off tests were conducted according to the ASTM D7522 (2015). A total of 12 pull-off tests were conducted in bonded areas identified with acoustic sounding. One pull-off test per FRP row was conducted at locations away from edges, to avoid areas that may have contained higher stress concentrations. Although EBFRPs retrofitted to columns are considered contact-critical and do not require a strong bond between the EBFRP and the concrete substrate as is needed in bond critical applications, the EBFRP material used to retrofit the columns was the same material used in bond critical applications and only bonded areas of the EBFRP retrofitted column were evaluated. In short, the test procedure consisted of: (1) sanding the EBFRP surface to remove any paint or coatings followed by cleaning with acetone to eliminate surface contamination; (2) adhering 5-cm aluminum pucks to the prepared test area using a quick-set epoxy adhesive; (3) coring the EBFRP around the perimeter of each puck with a 5-cm core-saw; (4) clamping the adhesion tester to the puck; and (5) applying a tensile load at a constant loading rate of approximately 335 N/s. The test setup is shown in Fig. 1 and the test procedure and failure modes evaluated were in accordance with ASTM D7522 (2015).

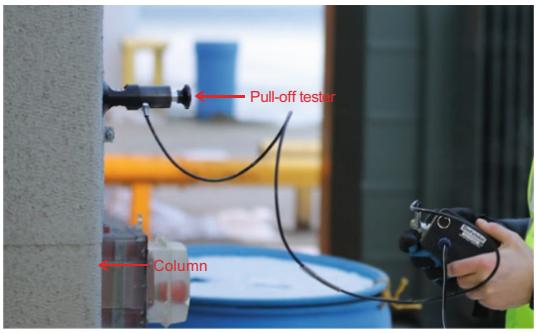

Fig. 1. Pull-off test setup

3.2 Phase 2: Materials Characterization

Differential scanning calorimetry (DSC) and *Attenuated Total Reflectance-Fourier Transform Infrared Spectroscopy* (ATR-FTIR) data were collected from CFRP and GFRP samples obtained from MKT and TSIA. Measurements were conducted at the Center for Composite Materials at the University of Delaware and the National Institute of Standards and Technology (NIST).

DSC was used to measure the glass transition temperature (T_g) values of the EBFRP samples to evaluate the effect surrounding temperature could have on the mechanical properties of the retrofit as well as the degree of polymer cross-linking density. The glass transition is the temperature range over which a polymer transitions from a solid to rubbery state, which is accompanied by decreased strength and stiffness. In DSC analysis, the EBFRP sample and a reference material (Fig. 2) are heated at the same rate in a temperature-controlled furnace, and the heat flow difference between the sample and reference is recorded. A step in the heat flow curve indicates the glass transition temperature range.

For DSC experiments, triplicate circular specimens with a mass between 8 mg and 16 mg were punched out from individual EBFRP samples using a press, and then placed into aluminum pans. To ensure seamless heat transfer between the pan and the material inside, mineral oil was used. The samples were covered with a pierced aluminum lid and sealed with a manual press. Each DSC experiment involved heating the samples from −20 °C to 250 °C at a constant heating rate of 10 °C/min under a nitrogen atmosphere. The T_g was determined as the midpoint temperature in the first heat run according to ASTM E1356 (2008).

ATR-FTIR spectroscopy was used to determine if any chemical degradation of the EBFRP composite retrofits had occurred over long-term outdoor exposure. ATR-FTIR spectroscopy is based on the interaction between infrared light and a sample. This technique relies on molecular vibrations in a sample to identify the presence of certain functional groups. A functional group absorbs infrared light if frequencies of the light and molecular vibrations are equal. As a result, a spectrum that shows absorbance as a function of wavelength is generated.

The spectra were collected using an FTIR spectrometer (Nicolet iS50 FTIR) with a diamond crystal ATR accessory. Each spectrum collected represents an average of 256 scans with a resolution of 4 cm^{-1}. ATR-FTIR spectra were baseline-corrected in Origin software. All spectra were normalized to the 1508 cm^{-1} band of the interior MKT sample corresponding to benzene ring stretching that was present across all spectra and is not expected to change with environmental exposure. At least three replicate areas per

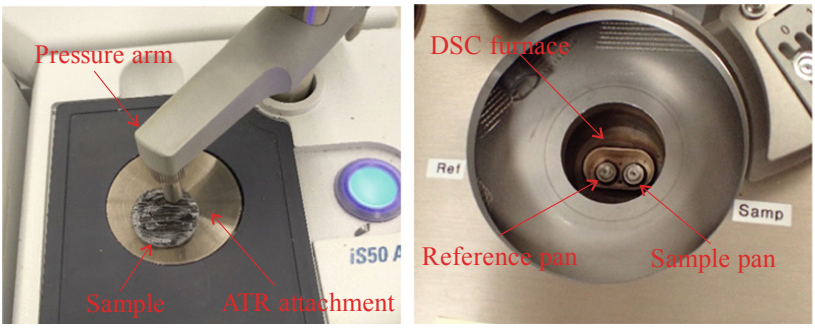

a) b)

Fig. 2. a) ATR-FTIR test setup, and b) sample inside DSC chamber.

sample were measured and the replicate spectra were averaged after baseline correction. The test setup is shown in Fig. 2.

4 Results and Discussion

Field assessment data acquired through visual inspection of eight representative buildings retrofitted with EBFRP showed no visible signs of earthquake damage to EBFRP composite retrofits. Figure 3a shows an example of an interior column at TSIA. Interior columns, wrapped with 2 plies of CFRP for confinement, were undamaged by the earthquake. For MKT, an exterior shear wall retrofitted with GFRP is shown in Fig. 3b. Wall boundary elements were formed by applying horizontally oriented unidirectional GFRP and CFRP on three sides of the window corner opening. Additional bolts were installed through the wall to confine the boundary elements. No obvious earthquake damage to the EBFRP retrofits was observed in the post-earthquake inspections. It should be noted that the team inspected only visible, exposed, EBFRP retrofits; during inspections of many of the buildings, the team faced accessibility problems as many EBFRP retrofits were located behind drywall, panels, or other architectural finishes.

a) b)

Fig. 3. Examples of typical EBFRP retrofits: a) interior column at TSIA; b) shear wall at MKT retrofitted with GFRP (marked by a dashed red line).

Acoustic sounding and Infrared (IR) thermography. Several debonded areas of varying size and shape were identified within the EBFRP composite system using acoustic sounding and the debonded areas were marked with tape. Qualitative IR thermography measurements were then taken and the debonded areas identified with tape were later matched up to IR thermography images (Fig. 4). On the interior column, thirteen relatively small debonded areas (between 10 cm^2 to 40 cm^2) were detected. In contrast, four larger debonded areas that exceeded 160 cm^2 were observed on the exterior column.

According to ACI 440.2R (2017), debonded areas larger than 160 cm^2 can affect the performance of EBFRP retrofits and should be repaired by selectively cutting away the affected sheet and applying an overlapping sheet patch of equivalent plies. It is unknown whether these debonded areas formed because of environmental deterioration, or due to construction defects. But, considering that debonding was more severe on the exterior column compared to the interior column and presuming that surface preparation and construction methods were the same between the columns, we conclude that environmental conditions likely had some influence on the EBFRP debonding in the exterior column. For field investigations, initial bond durability data would be useful as a baseline for researchers assessing bond quality after long-term outdoor exposure and hazard events.

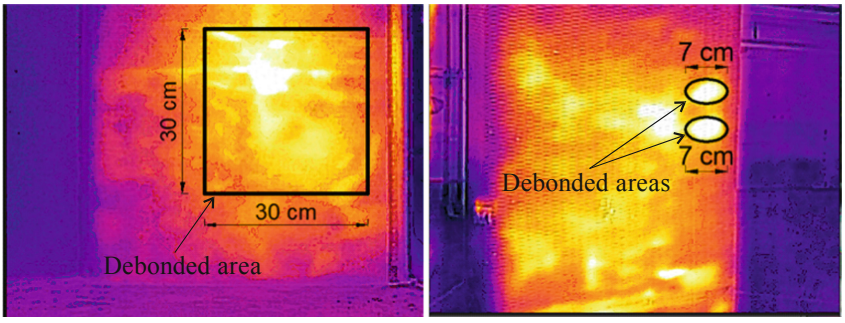

Fig. 4. Thermal IR image of debonding at TSIA: a) an exterior column and b) interior column. Bright areas were marked based on the location of tape from acoustic sounding.

Bond pull-off tests. Bond pull-off strengths were compared against the ACI 440.2R minimum bond strength requirement of 1.4 MPa (Fig. 5). Initial bond pull-off strength data was not available for any of the building components investigated. In future FRP retrofit installations, it would be useful to obtain and maintain this baseline data for long-term field inspections. Four different failure modes were observed in the bond pull-off tests (ASTM D7522): cohesive failure in the concrete substrate; adhesive failure at the EBFRP/concrete interface; mixed adhesive and cohesive failure; and, bonding adhesive failure at the loading fixture. Representative photographs of different failure modes are shown in Fig. 6. Cohesive failure in concrete (Fig. 6a) is desirable as it indicates sound adhesion between EBFRP and concrete, while the failure modes in Fig. 6b and Fig. 6c indicate improper adhesion between EBFRP and concrete, which can be caused by improper concrete surface preparation, environmental conditioning, or a combination of the two. Bonding adhesive failure at the loading fixture (Fig. 6d) occurred when the epoxy used to attach the fixture did not fully cure by applied heat in the extremely cold temperatures (<-12 °C) experienced during inspection. This failure mode was a non-result and was mostly avoided during subsequent pull-off tests on the same building component by applying heat for a longer period of time. Pull-off test strength data for this failure mode was not useful and is thus not included in Fig. 5.

At TSIA, measured bond pull-off strengths, both on the exterior and interior columns, were lower than the minimum requirement. Of note, pull-off bond strengths measured on the exterior column were lower compared to the interior column. Furthermore, two adhesive failures at the EBFRP-adhesive interface, which is an indication of poor bond properties, were recorded for the exterior column. The lower bond pull-off strengths on the exterior column at TSIA and the presence of adhesive failure modes provide evidence that there are some issues in regard to the durability of the bond between the CFRP and concrete.

All pull-off tests at MKT passed the 1.4 MPa minimum bond strength recommendation. Cohesive failure modes were observed in all experiments (with the exception of one bonding adhesive failure of the fixture on the exterior of the building) indicating good adhesion properties between the GFRP and concrete. Better bond performance observed at MKT in comparison to TSIA could be due to the mismatch in coefficients of thermal expansion (CTE) between the concrete and CFRP at TSIA. Carbon fibers have a negative CTE which leads to expansion under low ambient temperatures and, consequently, differential movement between the concrete and the EBFRP. On the other hand, the CTE of glass fibers is similar to the CTE of concrete, resulting in compatible deformations.

Several limitations should be noted for bond degradation assessment. First, with pull-off tests, the sample size was small due to the number of loading fixtures available at the time of this study and the cold weather issues that led to some bonding adhesive failures at the loading fixture. Further investigation of pull-off tests using a larger sample size is underway using data from a return trip to Anchorage. In future studies, improved statistical analysis can be accomplished using at least three pull-off tests per building component, with more pull-off tests conducted if inconsistencies are observed.

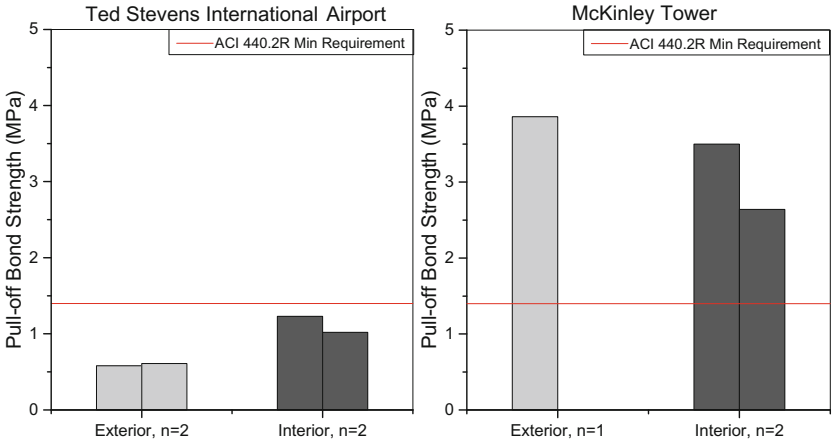

Fig. 5. Bond pull-off test strengths for all failure modes except bonding adhesive failure at the loading fixture. Each bar represents one pull-off test strength and the red line indicates the minimum bond pull-off test strength according to ACI 440.2R. Only one replicate was possible for the MKT exterior at the time of this field study because of a bonding adhesive failure at the loading fixture for the first pull-off test conducted.

Investigation of more than one building component should also be considered when it is possible in the field, and this approach was taken on our return trip to Anchorage. In comparison to the IR thermography technique, pull-off tests had the disadvantage of being destructive and sometimes led to inconsistent results. However, IR thermography had a longer measurement time and yielded false positives from thickened adhesive regions. Nevertheless, IR thermography could be validated with acoustic sounding and less localized results could be obtained with IR thermography compared to the highly localized results obtained with pull-off tests. Overall, a balanced approach with multiple techniques can help validate the findings of each individual technique.

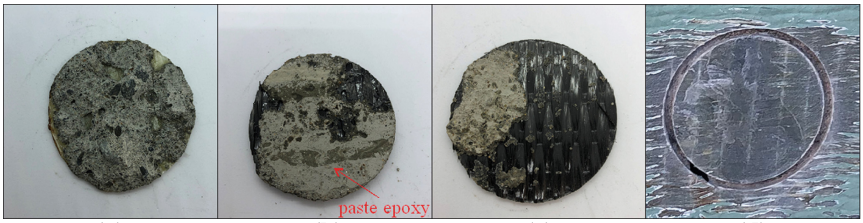

Fig. 6. Typical bond pull-off test failure modes: a) cohesive failure in the concrete substrate, b) adhesive failure at the EBFRP/concrete interface, c) mixed adhesive and cohesive failure mode, and d) bonding adhesive failure at the fixture-EBFRP interface.

Thermal analysis – The average T_g values obtained for CFRP retrofits from the interior and exterior column at TSIA are shown in Fig. 7. The observed T_g values for exterior CFRP retrofits at TSIA were in the 56 °C to 58 °C range. Interior retrofits at TSIA had lower T_g values which varied from 47 °C to 56 °C. The T_g values were likely greater for the exterior samples since higher outside temperatures during the summer season may have stimulated post-curing of the epoxy, leading to more cross-linking density.

The T_g values of GFRP samples from MKT were in the 53 °C to 54 °C range with no statistically significant difference between interior and exterior samples. During the service life of GFRP samples from MKT, the highest interior and exterior ambient temperatures most likely reached similar values as a result of less strictly controlled ambient conditions typical for residential buildings. Taking into account this assumption, similar values of measured T_g on the interior and exterior of MKT, can be attributed to a similar degree of post-curing.

According to ACI 440.2R, for a dry environment, it is suggested that the anticipated maximum service temperature of an EBFRP system not exceed (T_g – 15 °C). ACI 440.2R guidelines do not recommend specific service temperatures for different climatic areas, leaving it up to the licensed designed professional to specify the maximum service temperature. In this study, the maximum interior service temperature was conservatively assumed to be 30 °C for TSIA and MKT. The maximum service temperature for exterior applications was assumed to be 55 °C based on the literature (Michels et al. 2015). In the referenced study, the measurements performed on a pedestrian bridge in Switzerland, directly exposed to direct sunlight, show that the surface temperature was 55 °C

which was significantly greater than the measured ambient temperature on the day of the measurement (33 °C).

The minimum recommended exterior T_g (55 °C + 15 °C), based on the previously described exterior service temperature and the ACI 440.2R recommendation, was compared to the measured T_g values at MKT and TSIA. The measured T_g values of the exterior samples did not satisfy the minimum criteria from ACI 440.2R, for the suggested exterior service temperature of 55 °C, which may have adversely affected the mechanical properties of the EBFRP retrofits. In contrast, the measured interior T_g values were greater than the recommended minimum interior T_g (30 °C + 15 °C) which indicates that there was no impact of T_g on the mechanical properties of the interior EBFRP retrofits at both MKT and TSIA.

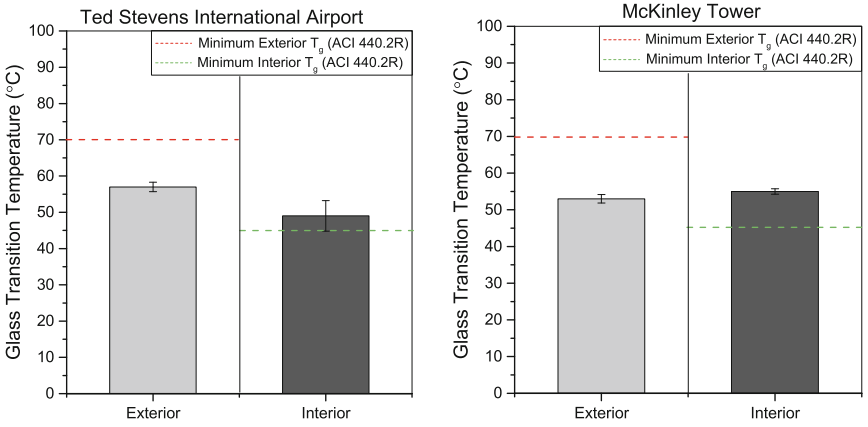

Fig. 7. The average T_g values of triplicate (8 mg to 16 mg) circular punched-out EBFRP specimens from individual samples collected at MKT and TSIA (error bars indicate one standard deviation). The minimum interior and exterior values indicate the threshold at which the T_g value of the EBFRP must exceed to maintain optimal mechanical properties.

ATR-FTIR. Typical spectra collected on the exterior and interior EBFRP samples are shown in Fig. 8. The peaks at 2920 cm^{-1} and 2850 cm^{-1} are related to C–H bonds of the monomer units, the peak at 1245 cm^{-1} corresponds to C-O bonds in epoxy, the peak at 1510 cm^{-1} corresponds to benzene ring, and the broad peak at 3370 cm^{-1} is related to hydroxyl groups (Cysne Barbosa et al. 2017). The band at 1730 cm^{-1}, when present in the spectra, corresponds to the carbonyl group and can indicate oxidation (Rezig et al. 2006).

The results suggest that the epoxy matrix at TSIA did not chemically change due to the field exposure to the subarctic climate: the spectra are qualitatively similar between the interior and exterior sample. Further analysis is underway with newly collected CFRP samples from TSIA to determine if any chemical changes are present among several other retrofitted columns. For the exterior EBFRP sample from MKT, the glass fibers were poorly saturated with epoxy, making it difficult to investigate epoxy degradation. There were some dissimilarities in peaks and peak intensities between the interior and exterior GFRP samples. The exterior GFRP sample was thought to be contaminated—the peaks

around 3680 cm^{-1} likely correspond to silica sand particles in the paste adhesive that was used to bond the EBFRP to the concrete substrate. The carbonyl peak at 1730 cm^{-1} was also present in the samples; the research team is currently conducting additional experiments to determine whether this peak is associated with oxidation of the epoxy matrix or is caused by contaminants that may have been present in the specimen (*e.g.*, paint). Further analysis is underway with newly collected GFRP samples from MKT exterior.

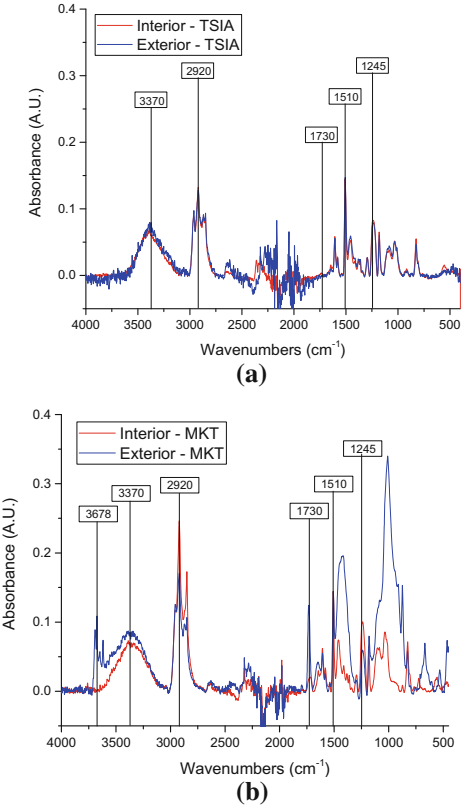

Fig. 8. Qualitative comparison of spectra on exterior and interior EBFRP from: a) TSIA, and b) MKT. Each spectrum is the average of three spectra from different areas of the same EBFRP sample. Bands of interest are denoted in boxes with units of cm^{-1}.

5 Summary and Conclusions

The primary objective of this work was to provide information on the performance of EBFRP retrofits in the 2018 earthquake in Anchorage, AK and the durability of EBFRP retrofits after long-term exposure to Alaska's sub-arctic climate. EBFRP retrofits at two concrete structures, the McKinley Tower and Ted Stevens International Airport,

retrofitted in 2004 and 2008, respectively, were investigated. Field assessment and laboratory testing of CFRP and GFRP samples collected from the buildings were performed. Field assessment included visual inspection to evaluate visible post-earthquake damage, IR thermography and acoustic sounding to detect debonded areas, and bond pull-off tests to evaluate the EBFRP-concrete bond quality. EBFRP material samples were collected during site visits to conduct DSC measurements to determine the glass transition temperature of the polymer matrix, and ATR-FTIR measurements to identify possible chemical degradation in the composite samples. Based on the experimental results presented in this paper, the following conclusions were made:

- No apparent signs of earthquake damage to EBFRP-retrofitted components were observed. Considering that many structural elements were located behind drywalls, visual inspection was not always possible. IR thermography and bond pull-off tests indicated that bond degradation may have occurred on exterior retrofits. It is not possible to draw firm conclusions about bond degradation without baseline data regarding the original quality of the bond and with the small sample size of pull-off tests. On a return trip to Anchorage, a larger sample size of three bond pull-off tests per column for multiple columns was accomplished, with more tests conducted when inconsistencies were observed. Further analysis of this data is underway.
- IR thermography required validation of debonded areas with acoustic sounding and was a time-consuming process. However, it was not destructive like pull-off testing and was more representative of the total column area. Overall, the use of multiple techniques can help validate the results of each individual technique and account for its limitations.
- Interior T_g values passed the minimum recommended T_g value per ACI 440.2R. However, T_g values measured on exterior EBFRP retrofits were below the minimum recommended temperatures.
- ATR-FTIR analysis shows that the polymer matrix in TSIA samples did not qualitatively changed during long-term exposure to environmental conditions in Alaska. GFRP samples from MKT showed the possible presence of contaminants in the spectra. Further investigation is underway with newly collected GFRP samples to verify the findings.

Acknowledgements. The authors gratefully acknowledge the funding provided by the United States National Science Foundation under the award number 1916972.

***Disclaimer*:** Certain commercial products or equipment described in this paper are present in order to adequately specify the experimental procedure. In no case does such identification imply recommendation or endorsement by the National Institute of Standards and Technology, nor does it imply that it is necessarily the best available for the purpose.

References

ACI 440.2R (2017) Guide for the Design and Construction of Externally Bonded FRP Systems for Strengthening Concrete Structures. American Concrete Institute, Farmington Hills

ASTM D7522 (2015) Standard Test Method for Pull-Off Strength for FRP Bonded to Concrete Substrate. ASTM International, West Conshohocken
ASTM E1356 (2008) Standard Test Method for Assignment of the Glass Transition Temperatures by Differential Scanning Calorimetry. ASTM International, West Conshohocken
Bakis CE et al (2002) Fiber-reinforced polymer composites for construction - state-of-the-art review. J Compos Constr 6(2):73–87
Brown JR (2005) Infrared Thermography Inspection of Fiber-Reinforced Polymer Composites Bonded to Concrete. PhD Dissertation, University of Florida, Gainesville
Buchan PA, Chen JF (2007) Blast resistance of FRP composites and polymer strengthened concrete and masonry structures - a state-of-the-art review. Compos B Eng 38(5–6):509–522
Cysne Barbosa AP et al (2017) Accelerated aging effects on carbon fiber/epoxy composites. Compos B Eng 110:298–306
Ehsani M (2017) Fiber Reinforced Polymers: Seismic Retrofit of the McKinley Tower. Structure Magazine
Goodwin DG, Sattar S, Dukes JD, Kim JH, Sung LP, Ferraris CC (2019) Research Needs Concerning the Performance of Fiber Reinforced (FR) Composites Retrofit Systems for Buildings and Infrastructure. Special Publication (NIST SP), p 1244
Hamilton HR, Brown J, Tatar J, Lisek M, Brenkus NR (2017) Durability Evaluation of Florida's Fiber-Reinforced Polymer (FRP) Composite Reinforcement for Concrete Structures. Florida Department of Transportation
He R, Yang Y, Sneed LH (2015) Seismic repair of reinforced concrete bridge columns: review of research findings. J Bridg Eng 20(12):04015015
ICRI-No.03732 (1997) Selecting and Specifying Concrete Surface Preparation for Sealers, Coatings, and Polymer Overlays. International Concrete Repair Institute, Des Plaines
Ma CK et al (2016) Repair and rehabilitation of concrete structures using confinement: a review. Constr Build Mater 133:502–515
Michels J, Widmann R, Czaderski C, Allahvirdizadeh R, Motavalli M (2015) Glass transition evaluation of commercially available epoxy resins used for civil engineering applications. Compos B Eng 77:484–493
National Oceanic and Atmospheric Administration: National Weather Service (2020). https://www.nws.noaa.gov/climate.php/xmacis.php%3Fwfo=pafc
Reay JT, Pantelides CP (2006) Long-term durability of state street bridge on interstate 80. J Bridg Eng 11(2):205–216
Rezig A et al (2006) Relationship between chemical degradation and thickness loss of an amine-cured epoxy coating exposed to different UV environments. J Coat Technol Res 3(3):173–184
Sheikh SA, Tam S (2007) Effect of freeze-thaw climatic conditions on long-term durability of FRP strengthening systems. Ministry of Transportation of Ontario, HIIFP-037
Steckel GL, Hawkins GF (2005) The Application of Qualification Testing, Field Testing, and Accelerated Testing for Estimating Long-Term Durability of Composite Materials for Caltrans Applications. Engineering and Technology Group The Aerospace Corporation, El Segundo
StEER (2018) Structural Extreme Event Reconnaissance Network and Earthquake Engineering Research Institute (EERI). Alaska Earthquake Preliminary Virtual Assessment Team (P-VAT) Joint Report
Tatar J, Hamilton HR (2014) Comparison of laboratory and field environmental conditioning on FRP-concrete bond durability. Constr Build Mater 122:525–536
Tatar J, Wagner D, Hamilton HR (2016) Structural testing and dissection of carbon fiber-reinforced polymer-repaired bridge girders taken out of service. ACI Struct J 113(6)
Zhang Y, Adams RD, Da Silva LFM (2014) Effects of curing cycle and thermal history on the glass transition temperature of adhesives. J Adhes 90(4):327–345